A Predictive Greenhouse Digital Twin for Controlled Environment Agriculture

Abdellah Islam Kafi[a], Antonio P. Sanfilippo[b], Raka Jovanovic[c] and Sa'd Abdel-Halim Shannak[d]

Qatar Environment and Energy Research Institute, Hamad Bin Khalifa University, Doah, Qatar
{*akafi, asanfilippo, rjovanovic, sshannak*}*@hbku.edu.qa*

Keywords: Digital Twin, Controlled Environment Agriculture, Time Series Forecasting, Machine Learning, Crop Yield Modeling, Edge Implementation.

Abstract: Controlled environment agriculture offers significant advantages for the efficient use of resources in food production, especially in hot desert climate regions due to the scarcity of arable land and water. However, farming practices such as hydroponics and aquaponics have high energy requirements for temperature control and present higher operational complexity when compared to traditional forms of farming. This study describes a Predictive Greenhouse Digital Twin (PGDT) that addresses these challenges through a dynamic crop yield assessment. The PGDT uses greenhouse measurements gathered through an IoT sensor network and a regression approach to multivariate time series forecasting to develop a model capable of predicting final crop yield as a function of the gathered measurements at any point in the crop cycle. The performance of the PGDT is evaluated with reference to forecasting algorithms based on deep and ensemble learning methods. Overall, deep learning methods show superior performance, with Long short-term memory (LSTM) providing a marginal advantage compared to Deep Neural networks (DNN). Furthermore, the models were deployed on an edge device (a Raspberry Pi-based gateway), where DNN demonstrated faster inference while delivering performance better than LSTM.

1 INTRODUCTION

As climate change keeps driving desertification through land degradation (Sivakumar, 2007) (Huang et al., 2020), food crop production becomes increasingly challenging, especially in hot desert climate regions due to the scarcity of water and arable land. For example, only 2.6% of Qatar's land was allocated to food production in 2019 (Planning and Authority, 2021) and only a small portion of the already scarce ground water is suitable for crop irrigation due to the presence of total dissolved solids concentration levels which are not suitable for food crops (Sanfilippo et al., 2024). Hydroponic and aquaponic farming alleviate these impediments through soil-less farming and significant reduction of water use but have high energy requirements for temperature control and present higher operational complexity when compared to traditional forms of farming (Sanfilippo et al., 2024). Both problems can be addressed through the development of a Predictive Greenhouse Digital Twin (PGDT) that can help identify the most efficient, profitable and sustainable use of resources in achieving the highest crop yields.

The PGDT presented in this study provides the basis for the automatic identification of economically sustainability in indoor farming through dynamic assessment of crop yield at any stage during the production cycle. The PGDT uses greenhouse measurements from a IoT sensor network and a regression approach to multivariate time series forecasting to provide a model capable to predict crop productivity as a function of the collected measurements. The integration of the PGDT with multi-objective optimization and technoeconomic analysis components can then be used to identify ideal trade-offs in the use of resources such as electricity, water and nutrients, and evaluate the economic sustainability of the ensuing trade-off scenarios as discussed in (Sanfilippo et al., 2024). The performance of the PGDT is evaluated with reference to three forecasting algorithms, two based on deep learn-

[a] https://orcid.org/0000-0001-8523-3492
[b] https://orcid.org/0000-0001-7097-4562
[c] https://orcid.org/0000-0001-8167-1516
[d] https://orcid.org/0000-0002-6842-7479

Kafi, A. I., Sanfilippo, A. P., Jovanovic, R. and Shannak, S. A.-H.
A Predictive Greenhouse Digital Twin for Controlled Environment Agriculture.
DOI: 10.5220/0013479900003929

In *Proceedings of the 27th International Conference on Enterprise Information Systems (ICEIS 2025) - Volume 1*, pages 980-987
ISBN: 978-989-758-749-8; ISSN: 2184-4992

ing methods (Deep Neural networks (DNN) and Long short-term memory (LSTM)) and the third based on the eXtreme Gradient Boosting algorithm (XGBoost).

The paper is structured into five sections. First, a review of the background literature on crop yield modeling is provided to highlight the contribution of the present study. Then the data used in this study and their sources are discussed. Next, the methodology used in the development of the PGDT is described and finally the results are presented. The paper concludes with a discussion of next steps with specific reference to integration with the multi-objective optimization and techno-economic analysis components.

2 BACKGROUND

Work on PGDTs as predictive models of greenhouse productivity can be grouped into two main categories according to whether first principle models or machine learning algorithms are used.

An example of PGDT based on first principle models is presented in (Sanfilippo et al., 2024) using the greenhouse micro-climate and tomato yield models developed in (Vanthoor et al., 2011b) and (Vanthoor et al., 2011a). The greenhouse micro-climate includes equations that compute the impact of factors relative to climate control in the greenhouse such as the insulation properties of the plastic sheeting covering the greenhouse, ventilation, the absorption of near-infrared radiation, plant transpiration rate, and fluxes generated by the plants' canopy activity. The tomato growth model employs a shared carbohydrate buffer that handles the distribution to plant organs and is primarily influenced the micro-climate model, as shown in Figure 1.

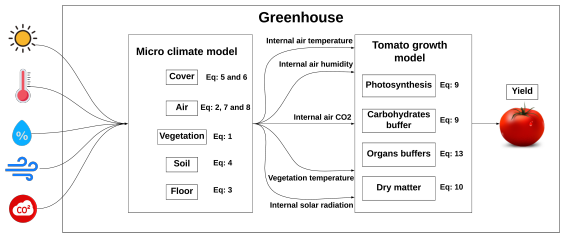

Figure 1: Example of PGDT based on a first principles model (Sanfilippo et al., 2024).

Most PGDTs based on machine learning make use of neural network algorithms. One of the earliest studies (Ehret et al., 2011) provides a neural network model of greenhouse tomato yield, growth and water use from automated crop monitoring data. The study described in (Qaddoum et al., 2013) used fuzzy neural networks to model tomato yield. The authors in (Alhnaity et al., 2019) make use of a long short-term memory neural network algorithm to model plant growth in greenhouses and show that the model developed outperforms support vector regression and random forest algorithms. The authors in (Gong et al., 2021) present a greenhouse crop yield prediction model that combines temporal convolutional and recurrent neural networks and rivals traditional machine learning approaches such as linear regression, random forest, support vector regression, decision tree, gradient boosting, and multi-layers artificial neural network. These studies all represent significant advanced in modeling crop growth in a greenhouse environment. Our study contributes to this endeavor through the comparison of deep learning algorithms with the eXtreme Gradient Boosting algorithm (XGBoost).

3 DATA

The data used in this study include meteorological measurements outside the greenhouse monitored through the National Solar Radiation Database (NSRD) (https://nsrdb.nrel.gov) and measurements from a hydroponic tomato greenhouse at the Agrico Agricultural Development (https://agrico.qa). Greenhouse measurements were gathered through a network of IoT sensors installed in the hydroponic tomato greenhouse throughout a full tomato growth cycle, early November 2023 through the end of May 2024. These include electrical soil conductivity (EC), luminosity (LUX), soil temperature (S_TEMP), relative humidity (RH), air temperature (TEMP), pH, and harvest quantities, as shown in Tables I and II. Harvest quantities were manually recorded and provide the key indication of crop yield. For additional details on the greenhouse characteristics and the IoT sensor network see (Sanfilippo et al., 2024).

4 METHODOLOGY

The primary objective of this study is to assess and compare the performance of three distinct forecasting algorithms, DNN, LSTM, and XGBoost, in predicting crop yield. A methodical approach was employed for data collection, preprocessing, model development, training procedures, and performance evaluation. The most adequate models were chosen for implementation on an edge device to enable immediate yield forecasting in the greenhouse environment. The approach included transforming the trained models into compact formats appropriate for edge deployment and utilizing quantization methods to minimize the models'

memory usage and inference delay. The implementation setup was integrated with the existing IoT sensor network, allowing seamless data flow.

4.1 DNN, LSTM and XGBoost

The architecture of DNNs (Sze et al., 2017) comprises input, hidden and output layers. The input layer receives data. The hidden layers consist of interconnected nodes where data inputs are associated with weights. Each node computes the weighted sum of its inputs and passes the results through an activation function. Activated nodes are summed and passed through to the output layer as predictions. During training, forward and backward propagation steps operate on training data records. In forward propagation, data are fed into the input layer, passed through each hidden layer, and the network's prediction is generated from the final output layer. In backward propagation, the network's prediction is compared to the observed value, the ensuing error is propagated backward through the network layer by layer, and the weights of the connections between nodes are adjusted using algorithms such as gradient descent to minimize the error.

Differently from DNNs, an LSTM (Hochreiter, 1997) is structured as a network of cells. Each cell contains a memory component, a forget gate, an input gate and an output gate. After the LSTM cell receives input data, the forget gate determines which information from the previous step is to be discarded and the input gate determines which new information should be stored in memory. A new candidate value is computed using the previous hidden state of the network, the current input, and the input gate. The memory cell is updated by combining the old memory cell content with the new candidate value, weighted by the forget gate and input gate values, respectively. The output gate decides how much of the updated memory cell content should be used to compute the output of the cell. The final output of the LSTM cell is computed by multiplying the output gate value with the updated memory cell content.

In XGBoost (Chen and Guestrin, 2016) weak learners are iteratively combined to minimize the ensemble error. The model is initialized with a weak learner, e.g., a decision stump model (Iba and Langley, 1992), which is evaluated on the reference dataset to compute residuals using a loss function such as the Mean Squared Error (MSE). Then, a new weak learner is built that minimizes the loss function by fitting the new weak learner to the dataset with the objective of predicting both the first and second order gradients of the loss function from the previous weak learner. Finally, the ensemble model is updated by adding a scaled version of the weak learner's prediction. This process is repeated until the optimal results are achieved and the final model is derived as the weighted mean of all weak learners.

Table 1: Harvest quantities time series sample.

Date	*Harvest Quantities (Kg.)*
01/03/24	21
01/06/24	80
01/06/24	27
01/06/24	6
01/08/24	200
01/08/24	22
01/08/24	1
...	...

Table 2: Parameters measured in near real-time and aggregated daily.

Date	*EC*	*LUX*	*S_TEMP*	*RH*	*TEMP*	*pH*
06/11/23	0.7	8971.3	27.4	61.6	26.1	4.3
07/11/23	0.9	11891.4	26.7	61.1	26.4	4.9
...	...	...	...	...	...	...

4.2 Data Wrangling

Before training and evaluating the DNN, LSTM and XGBoost forecasting algorithms on the reference dataset, the relation in time and frequency granularity between the dependent variable, i.e., harvest quantities, and the independent variables, i.e., EC, LUX, S_TEMP, RH, TEMP, and pH, in the dataset need to be normalized. Harvest quantities are typically distributed unevenly through the production cycle, with no output in the initial period of growth (i.e, early November through early January in Qatar), multiple or single collections of varying quantities in a single day, and intervening days with no collection, as shown in Table (1), while other parameters are measured in near real-time and aggregated daily as shown in Table (2). So, while there are data points for every day of the crop growth cycle (209 days) for the independent variables, there are only 101 data points for the dependent variable (i.e., harvest quantities) that represent a total of 37 days taking into account days of repeated harvesting.

We employed a sliding window technique to capture the temporal dependencies inherent in greenhouse sensor data during feature engineering. This method involves creating subsets of consecutive data points, where each subset (or window) contains a fixed number of time steps—in this case, eight days. For every window, the corresponding input features are aggregated to form a feature vector representing the greenhouse's state over the preceding eight-day

period. Specifically, each window includes measurements of EC, LUX, HUM, TEMP, YIELD, and the number of days since the start of the plantation cycle. The target variable for each window is the yield value following the window period. By sliding this window across the entire dataset, we generated many training samples that enabled the models to learn patterns and trends associated with crop growth and yield fluctuations.

We employed a forward-filling method to assign missing yield values to address the non-daily recording of harvest quantities. Specifically, after a harvest event was recorded on a particular day, the corresponding yield value was carried forward and assigned to all subsequent days until the next harvest day. This technique assures that the yield data stays constant during periods without recorded harvests reflecting the real-world available information. By doing so, the model can leverage the most recent yield information when predicting future yields while minimizing the introduction of bias that could result from arbitrary interpolation.

4.3 Training and Testing

We explore the architecture design and training procedures employed for each predictive model integrated into the PGDT. We explore three distinct modeling approaches: DNN, LSTM, and XGBoost. Each model's architecture, hyperparameter configurations, and training methodologies are detailed to provide a comprehensive understanding of their implementation characteristics. The training was conducted on a Linux machine with an AMD Ryzen 7900 12-core processor, an NVIDIA RTX 4070 GPU with 12 GB of VRAM, and 32GB of DDR4 RAM. During training, the DNN and LSTM models were trained on the GPU. The XGBoost model, implemented using the XGBoost library, was trained on the CPU.

4.3.1 Deep Neural Network

The DNN model begins with an input layer that accepts data sequences with eight-time steps window size. Subsequently, these multidimensional inputs are flattened into a single vector to facilitate processing by the dense layers. The DNN comprises two fully connected hidden layers containing 256 neurons with ReLU activation functions.

Training the DNN involved using the Adam optimizer with a learning rate 0.001, aiming to minimize the Mean Squared Error (MSE) loss function. The model was trained over 100 epochs with a batch size of 32. TimeSeriesSplit with eight splits was employed for cross-validation, maintaining the chronological integrity of the time series data. Feature scaling was performed using the MinMaxScaler, which normalized the input features to a range between 0 and 1.

4.3.2 Long Short-Term Memory Network

The LSTM architecture begins with an input layer that processes sequences of eight-time steps, each comprising six features similar to the DNN model. This input is fed into a stack of LSTM layers, each containing 256 memory units.

Each LSTM layer is equipped with dropout regularization, although the current configuration sets the dropout rate to 0.2 to control overfitting. The output is a dense layer with a linear activation function, generating the predicted yield value.

Training the LSTM model utilized the Adam optimizer with a learning rate 0.001 and aimed to minimize the MSE loss function. The model was trained for 100 epochs with a batch size of 32, TimeSeriesSplit with eight splits for cross-validation, and feature scaling was similarly performed using the MinMaxScaler to normalize input features.

4.3.3 eXtreme Gradient Boosting

The XGBoost architecture was configured with a learning rate of 0.1, 200 estimators, and a maximum tree depth of six. Additionally, a subsample ratio of 0.8 was employed by randomly sampling 80% of the training data for each tree. These hyperparameters were selected to balance model complexity and generalization performance.

Training the XGBoost model involved fitting the algorithm to the scaled training data using the MinMaxScaler to normalize the input features. The model was trained over 200 boosting rounds with a learning rate of 0.1, and it was optimized based on the gradient of the loss function.

4.3.4 Evaluation Procedures

Each model's performance was evaluated using key metrics, including ,

Root Mean Squared Error (RMSE),

$$\text{RMSE} = \sqrt{\frac{1}{n}\sum_{i=1}^{n}(y_i - \hat{y}_i)^2},$$

coefficient of determination (R^2),

$$R^2 = 1 - \frac{\sum_{i=1}^{n}(y_i - \hat{y}_i)^2}{\sum_{i=1}^{n}(y_i - \bar{y})^2},$$

and Mean Absolute Error (MAE),

$$\text{MAE} = \frac{1}{n}\sum_{i=1}^{n}|y_i - \hat{y}_i|.$$

These metrics comprehensively assess each model's accuracy and generalization capability.

Furthermore, Mean Squared Error (MSE) is used for the loss function and given by:

$$\text{MSE} = \frac{1}{n}\sum_{i=1}^{n}(y_i - \hat{y}_i)^2,$$

Where:

- y_i is the actual value,
- $\hat{y}_i$ is the predicted value,
- $\bar{y}$ is the mean of the actual values,
- n is the number of observations.

5 RESULTS AND DISCUSSION

The experimental evaluation of the PGDT highlights different performance aspects among the DNN, LSTM, and XGBoost models when forecasting greenhouse tomato yields using the time series dataset described in Section 3. This section presents an in-depth discussion of the comparative performance of these methods.

Figure 2 illustrates the actual versus predicted yields for each model across the whole crop cycle, catching both the beginning of fruit production and the peak yield phase. Although all models exhibit a general upward trend, their fidelity to ground truth varies substantially, especially near the peak yield phase.

Generally, Figure 2 demonstrates that DNN and LSTM capture yield patterns. LSTM predictions align more robustly with the ground truth observations. XGBoost, despite its overall ability to follow the trend, always underestimates yield values. These initial observations are further quantified in the subsections below.

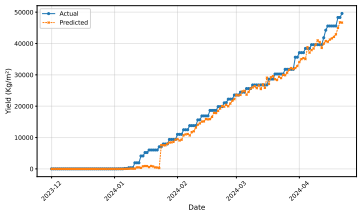

(a) DNN.

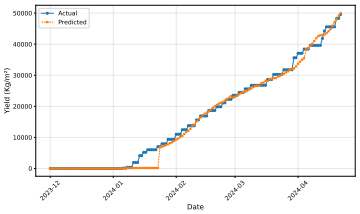

(b) LSTM.

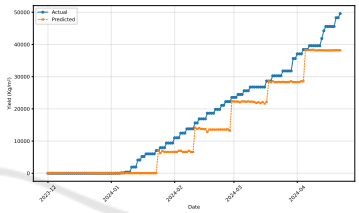

(c) XGBoost.

Figure 2: Actual vs. predicted yields.

5.1 Metrics Analysis

Key metrics are employed to evaluate predictive accuracy: MAE, RMSE, and (R^2).

LSTM achieves the lowest MAE (1,007.39 kg/m^2) and RMSE (1,769.86 kg/m^2), outperforming both DNN and XGBoost. These lower error values indicate that, on average, LSTM predictions remain closer to actual harvest quantities and that more significant prediction errors are less frequent.

Figure 3 shows the evolution of MAE across different folds, demonstrating the model stability with various data subsets. LSTM consistently achieves MAE values below 1,500 kg/m^2 across all folds, reflecting strong generalization. In contrast, the DNN

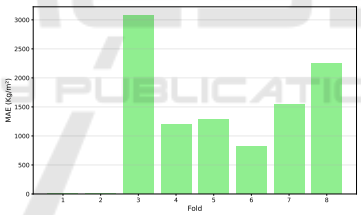

(a) DNN.

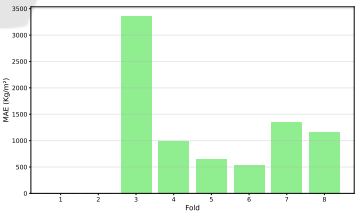

(b) LSTM.

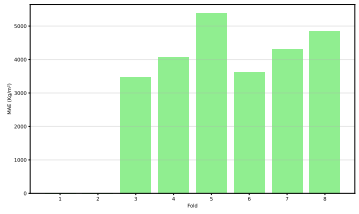

(c) XGBoost.

Figure 3: MAE progression across folds.

exhibits moderate fluctuations, with some folds rising to nearly 1,800 kg/m^2, implying sensitivity to particular training subsets. XGBoost, on the other hand, displays significant fluctuations, with errors exceeding 4,000 kg/m^2 in the later folds.

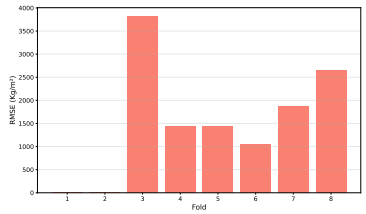

(a) DNN.

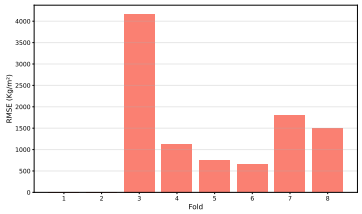

(b) LSTM.

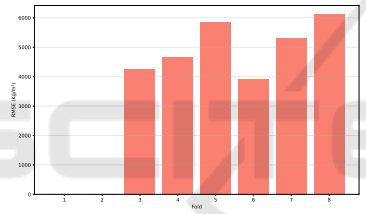

(c) XGBoost.

Figure 4: RMSE trends across folds.

The RMSE results, plotted in Figure 4, follow the MAE trends. DNN registers moderate RMSE fluctuations, while LSTM retains relatively low RMSE values across folds, showing its stable performance. XGBoost's errors are more than 5,000 kg/m^2, highlighting the model's low performance.

Evaluating the (R^2) metric, LSTM attains the highest score (0.986), slightly surpasses DNN (0.984), and noticeably outperforms XGBoost (0.916). Although the difference between LSTM and DNN appears small, an inspection of the time series predictions indicates a benefit during rapid transitions and peak yield phases.

Figure 5 underscores that while DNN and LSTM maintain relatively high R^2 values across folds, XGBoost occasionally drops into negative values, indicating that the model can, in particular data splits, perform worse than a simple mean-based predictor.

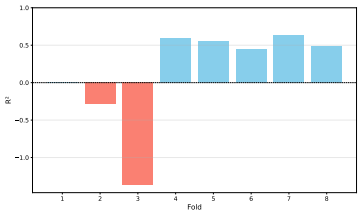

(a) DNN.

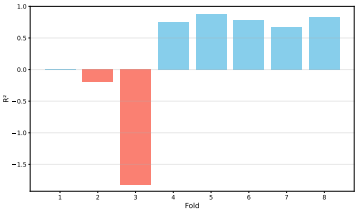

(b) LSTM.

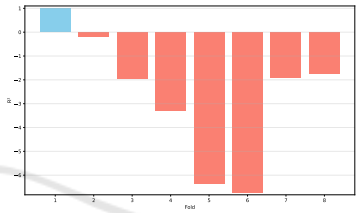

(c) XGBoost.

Figure 5: R^2 consistency. Negative values for XGBoost indicate failed generalization.

Table 3: Comparative Model Performance Metrics.

Metric	DNN	LSTM	XGBoost
MAE (kg/m^2)	1,270.08	1,007.39	3,213.78
RMSE (kg/m^2)	1,946.96	1,769.86	4,404.05
R^2	0.984	0.986	0.916

5.2 Edge Deployment

The final trained DNN and LSTM models were deployed on an edge device, specifically a gateway based on Raspberry Pi 4, to allow real-time yield prediction at the greenhouse level. This edge deployment guarantees localized processing of sensor data, reducing latency and dependence on cloud infrastructure while maintaining data privacy. The TensorFlow Lite framework was employed to convert the trained models into lightweight formats suitable for execution on the microcontroller boards.

Both models were quantized to the Float16 precision format during conversion to reduce their size and inference latency while maintaining nearly comparable accuracy to their full-sized counterparts. Quantization to Float16 reduces the memory footprint of the models, making them favorable for edge devices. After quantization, the size of the DNN model was

(a) The edge gateway device used to deploy the developed models.

(b) IoT sensor nodes installed inside the greenhouse for data collection.

Figure 6: Edge deployment setup comprising the gateway device and greenhouse sensor nodes.

reduced from 977 KB to just 160 KB and the LSTM model from 3.3 MB to 549 KB.

Once deployed, the Float16 quantized models processed real-time sensor data collected from the greenhouse and provided yield predictions with average inference times of approximately 0.000067 seconds for the DNN and 0.005009 seconds for the LSTM on the Raspberry Pi.

Table 4 summarizes the performance comparison between the quantized and full-sized models. Despite the significant reduction in size and latency, the quantized models performed nearly identical predictive metrics, including MAE, RMSE, and R^2, demonstrating their suitability for edge deployment.

Table 4: Performance Comparison: Full vs. Quantized Models.

Metric	DNN (Full / Quantized)	LSTM (Full / Quantized)
Model Size (KB)	977 / 160	3,300 / 549
RMSE(kg/m^2)	1,650.35 / 1,650.22	2,096.42 / 2,096.01
MAE(kg/m^2)	1,163.14 / 1,162.82	1,398.72 / 1,397.39
R^2	0.984 / 0.988	0.986 / 0.981

5.3 Performance Comparison for Edge Implementation

Table 5 compares the performance of the DNN and LSTM models on the edge device.

Table 5: Edge Deployment Performance Comparison.

Metric	DNN	LSTM
RMSE(kg/m^2)	1,650.22	2,096.01
MAE(kg/m^2)	1,162.82	1,397.39
R^2	0.9882	0.9810
Inference Time (s)	0.000067	0.005009

The results in Table 5 illustrate the trade-offs between the DNN and LSTM models when deployed on the Raspberry Pi 4. The DNN model exhibited faster inference times and slightly better performance across most metrics, including MAE, RMSE, and R^2.

Despite the Raspberry Pi's computational constraints, both models achieved real-time inference capabilities, making them suitable for edge deployment in controlled-environment agriculture.

6 CONCLUSIONS AND FURTHER WORK

In this study, we developed and evaluated a PGDT for hydroponic tomato production using three different forecasting techniques: DNN, LSTM, and XGBoost. Our outcomes show that LSTM consistently outperforms DNN and XGBoost across multiple error metrics.

DNN also demonstrates good performance while exhibiting slightly higher error rates. XGBoost trains rapidly, and its inconsistencies in yield prediction reduce its reliability for real-world applications.

To further evaluate the PGDTs, we deployed the models on an edge device (a Raspberry Pi-based gateway), allowing real-time decision-making at the greenhouse site without relying on cloud solutions. While LSTM demonstrated superior accuracy, DNN

emerged as a compelling alternative for edge deployment due to its significantly faster inference times and close performance to LSTM, making DNN a better candidate for edge implementation.

Next steps include further evaluation of the PGDT developed in this study using synthetic data and its integration with multi-objective optimization and techno-economic analysis components. First, we will develop a synthetic dataset using the greenhouse dataset described in this paper as training material with generative AI algorithms such as generative adversarial networks and variational auto-encoders and evaluate the reliance of the emerging forecasting model using metrics such as discriminative and predictive scores (Yoon et al., 2019) (Desai et al., 2021). Then, we will select the emerging best-in-class forecasting model as input to multi-objective optimization to develop a framework that helps farmers identify optimal resource trade-offs in securing robust crop yields following the approach described in (Sanfilippo et al., 2024). Finally, we will evaluate the economic sustainability of optimimal trade-off scenarios through techno-economic analysis, as discussed in (Sanfilippo et al., 2024).

ACKNOWLEDGEMENTS

The authors would like to acknowledge Nasser Al-Khalaf, Jovelyn Beltran, and Mohamed Batran at AGRICO for their collaboration with data and setup to conduct the study and test the systems. This work was supported by the Ministry of Municipality and Environment (MME) under Grant MME02-0911-200015 from the Qatar National Research Fund (a member of Qatar Foundation) / QRDIC. The findings herein reflect the work and are solely the responsibility of the authors.

REFERENCES

Alhnaity, B., Pearson, S., Leontidis, G., and Kollias, S. (2019). Using deep learning to predict plant growth and yield in greenhouse environments. In *International Symposium on Advanced Technologies and Management for Innovative Greenhouses: GreenSys2019 1296*, pages 425–432.

Chen, T. and Guestrin, C. (2016). Xgboost: A scalable tree boosting system. In *Proceedings of the 22nd acm sigkdd international conference on knowledge discovery and data mining*, pages 785–794.

Desai, A., Freeman, C., Wang, Z., and Beaver, I. (2021). Timevae: A variational auto-encoder for multivariate time series generation. *arXiv preprint arXiv:2111.08095*.

Ehret, D. L., Hill, B. D., Helmer, T., and Edwards, D. R. (2011). Neural network modeling of greenhouse tomato yield, growth and water use from automated crop monitoring data. *Computers and electronics in agriculture*, 79(1):82–89.

Gong, L., Yu, M., Jiang, S., Cutsuridis, V., and Pearson, S. (2021). Deep learning based prediction on greenhouse crop yield combined tcn and rnn. *Sensors*, 21(13):4537.

Hochreiter, S. (1997). Long short-term memory. *Neural Computation MIT-Press*.

Huang, J., Zhang, G., Zhang, Y., Guan, X., Wei, Y., and Guo, R. (2020). Global desertification vulnerability to climate change and human activities. *Land Degradation & Development*, 31(11):1380–1391.

Iba, W. and Langley, P. (1992). Induction of one-level decision trees. In *Machine learning proceedings 1992*, pages 233–240. Elsevier.

Planning, Q. and Authority, S. (2021). Qatar voluntary national review 2021. https://sustainabledevelopment.un.org/memberstates/qatar.

Qaddoum, K., Hines, E., and Iliescu, D. (2013). Yield prediction for tomato greenhouse using efunn. *International Scholarly Research Notices*, 2013(1):430986.

Sanfilippo, A., Kafi, A., Jovanovic, R., Ahmad, N., Wanik, Z., et al. (2024). Sustainable energy management for indoor farming in hot desert climates. *Sustainable Energy Technologies and Assessments*, 71:103958.

Sivakumar, M. V. (2007). Interactions between climate and desertification. *Agricultural and forest meteorology*, 142(2-4):143–155.

Sze, V., Chen, Y.-H., Yang, T.-J., and Emer, J. S. (2017). Efficient processing of deep neural networks: A tutorial and survey. *Proceedings of the IEEE*, 105(12):2295–2329.

Vanthoor, B., De Visser, P., Stanghellini, C., and Van Henten, E. J. (2011a). A methodology for model-based greenhouse design: Part 2, description and validation of a tomato yield model. *Biosystems engineering*, 110(4):378–395.

Vanthoor, B., Stanghellini, C., Van Henten, E. J., and De Visser, P. (2011b). A methodology for model-based greenhouse design: Part 1, a greenhouse climate model for a broad range of designs and climates. *Biosystems Engineering*, 110(4):363–377.

Yoon, J., Jarrett, D., and Van der Schaar, M. (2019). Time-series generative adversarial networks. *Advances in neural information processing systems*, 32.